DOI: 10.1002/anie.201106447

# Host–Guest Geometry in Pores of Zeolite ZSM-5 Spatially Resolved with Multiplex CARS Spectromicroscopy**

*Katrin F. Domke,* James P. R. Day, Gianluca Rago, T. Alexander Riemer, Marianne H. F. Kox, Bert M. Weckhuysen, and Mischa Bonn*

The geometrical arrangement of reagent molecules in the nanometer-sized pores of zeolite catalysts results from physicochemical interactions between reagent and catalyst, and plays a crucial role in determining the overall catalytic activity of the system.[1] Steric constraints, for example, lead to favored molecular geometries and diffusion paths into and out of the pores, which, in turn, may influence the reaction pathway. Intermolecular interactions compete with reagent–zeolite interactions, and the strength of these interactions is reflected in the spatial alignment of molecules in the zeolite pores. Thus, knowledge of the local molecular orientation inside a catalyst particle provides insight into the chemical functionality of the host–guest system and, ultimately, its macroscopic reactivity. Such knowledge is essential in attempts to design a catalyst with optimal activity.[2] A variety of experimental methods,[3] such as infrared, Raman, single- and two-photon fluorescence, UV/vis, and second harmonic generation (SHG) spectroscopy, as well as modeling approaches,[4] have been employed to determine the orientation of guest molecules inside zeolite pores. To understand the local reactivity of zeolites, however, spatially resolved imaging is required. Recently, 2D mapping of reagent ordering in zeolite pores was achieved with nonlinear fluorescence and SHG microscopy approaches,[5] both of which are based on probing electronic molecular resonances. On the other hand, multiplex coherent anti-Stokes Raman scattering (mCARS) microscopy has been used for vibrational imaging of molecular adsorption in zeolites.[6] In principle, this approach provides local information on host–guest geometry, host–guest chemical interactions, and the correlation between geometry and chemistry simultaneously.

[*] Dr. K. F. Domke, Dr. J. P. R. Day, G. Rago, T. A. Riemer, Prof. M. Bonn
FOM Institute AMOLF
Science Park 104, 1098 XG Amsterdam (The Netherlands)
E-mail: domke@amolf.nl
Prof. M. Bonn
Max Planck Institute for Polymer Research
Ackermannweg 10, 55128 Mainz (Germany)
Dr. M. H. F. Kox, Prof. B. M. Weckhuysen
University of Utrecht
Universiteitsweg 99, 3584 CG Utrecht (The Netherlands)

[**] K.F.D. thanks the Alexander von Humboldt Foundation (Germany) for a Feodor Lynen Fellowship. This work is part of the research program of the Stichting FOM with financial support from NWO. CARS = coherent anti-Stokes Raman scattering.
Supporting information for this article is available on the WWW under http://dx.doi.org/10.1002/anie.201106447.

Here, we show how the characterization of a sample in three dimensions and on the micron scale with mCARS provides detailed insight into reagent–catalyst geometry and interactions. We determined the highly anisotropic reagent arrangement and local chemical environment of 2-chlorothiophene (2CT) in zeolite ZSM-5 pores. This system is of fundamental interest for the development of novel catalytic desulfurization routes to reduce sulfur content in fuels to comply with increasingly strict environmental regulations.

Similar to spontaneous Raman spectroscopy, mCARS probes Raman-active vibrational modes of molecules, providing a chemical fingerprint of the species under investigation that reflects their interactions with the local environment. For a given molecule concentration, the scattering intensity of a vibrational mode depends on the orientation of the chemical bond relative to the polarization of the excitation beams. While spontaneous Raman spectroscopy is routinely employed to determine molecular orientation, the potential of mCARS to investigate molecular ordering has been explored only sporadically for biological systems.[7] Owing to its intrinsic capacity for micrometer-resolution sectioning in 3D and very high sensitivity, mCARS is particularly suited for the investigation of the local adsorption geometry and chemistry of reagent molecules in zeolite pore systems with high spatial resolution at short acquisition times. Throughout this work, we present Raman-like spectral responses which were retrieved from the original mCARS spectra with help of the maximum entropy method for the direct quantitative analysis of band intensities.[8] Zeolites H-ZSM-5 (Brønsted acidic sites (BAS) present) and Na-ZSM-5 (no BAS present) fully loaded with 2CT were investigated to examine the role that molecule–molecule and molecule–zeolite interactions play for molecular adsorption geometry (experimental details in the Supporting Information).

Figure 1 a shows a set of Raman responses of an H-ZSM-5 crystal loaded with 2CT. The curves were obtained with different orientations of the long edge of the crystal with respect to the laser polarization. The focus was located at a depth of 8 μm from the zeolite surface centered in $x,y$, viewing along the crystal's roof ridge. In the CH stretching region, intense Raman bands are found at −3122, −3110, −3100, and −3080 $cm^{-1}$, in addition to the C=C stretching mode at −1410 $cm^{-1}$ and the C–C stretching mode at −1345 $cm^{-1}$. In contrast, the Raman spectrum of liquid 2CT exhibits only three vibrational modes in the CH stretching region at −3112, −3097, and −3084 $cm^{-1}$ (spectra not shown), aside from similar C=C and C–C stretching frequencies at −1412 and −1347 $cm^{-1}$, in agreement with spontaneous Raman literature values.[9]

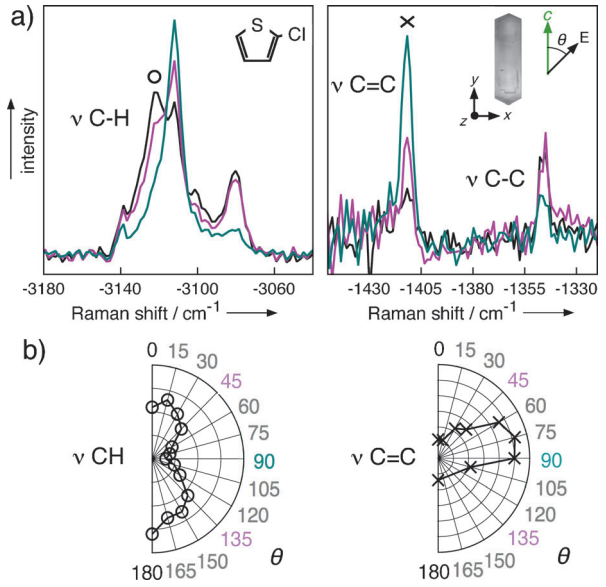


***Figure 1.*** Varying the angle $\theta$ between the crystal's *c* axis and the beam polarization results in changes in the Raman response of 2CT/H-ZSM-5. At $\theta = 0°$, the beam polarization is aligned perpendicularly to the straight pores. a) Selected spectra recorded at a depth of $z = 8$ µm centered in *x*,*y* in the CH and C–C stretching regions for $\theta = 0°$ (black), 45/135° (magenta), 90° (blue). Insets: Chemical structure of 2CT; beam polarization with respect to the *c* axis of crystal (white-light image of ZSM-5 crystal). b) Polar plots of the intensities of the −3122 and −1410 $cm^{-1}$ bands as a function of $\theta$.

We observe a strong dependence of the 2CT Raman signal on the orientation of the incident light polarization with respect to the crystal's *c* axis. Control experiments probing the stretching vibration of $N_2$ adsorbed isotropically in the zeolite pores, on the other hand, show no orientation dependence (Figure S1 in the Supporting Information). Hence, variations in the spectral intensity cannot be due to the crystal's birefringence, which was measured to be as low as 0.008, with an increase upon loading to about 0.028.[10] Importantly, no wavelength dependence of the birefringence was observed in the region of interest for our study between 700 and 900 nm.[10] Thus, we can also rule out that the observed spectral changes are due to changes in the beam polarizations with respect to each other; we expect to always probe $\chi^{(3)}_{1111}$. Our observations for 2CT must be explained in terms of molecular ordering.

The polar plots in Figure 1 b depict the behavior of two selected 2CT modes (all plots are given in Figure S2 in the Supporting Information). When the angle $\theta$ between the crystal's *c* axis and the beam polarization is varied from $\theta = 0°$ to $\theta = 90°$, the scattering intensity at −3122 $cm^{-1}$ drops, whereas that of at −1410 $cm^{-1}$ increases. The effect of crystal rotation on the band intensities is most pronounced for ν(C=C) at −1410 $cm^{-1}$ which shows a maximum near $\theta = 90°$. To a first approximation, the Raman tensor of ν(C=C) has its preferential polarizability along the bond axis.[11] Because the scattering intensity depends on the orientation of the bond relative to the beam polarization,[7b] the pronounced dipolar patterns indicate the molecular ordering of 2CT inside the pores. The observed Raman anisotropy, that is, band intensity ratio $I_{\theta=0}/I_{\theta=90}$, for the C=C stretching mode is found to be 4.3. This value is close to that of 5.5 found for highly ordered polythiophene films.[11] Assuming a uniaxial (and largely unperturbed by the presence of the zeolite) polarizability tensor of ν(C=C) for 2CT/ZSM-5 similar to that of polythiophene, the observed anisotropy value suggests a substantial degree of 2CT ordering.

As we observe identical behavior for 2CT adsorbed on H-ZSM-5 and Na-ZSM-5 (Figure S3 in the Supporting Information), we conclude that the alignment of the molecules and the chain orientation are independent of the presence of BAS. Apparently, the intermolecular interactions are stronger than the chemical interactions between 2CT and BAS under the given experimental conditions. Likely, the 1D molecular ordering in the adsorbed state of 2CT results in the appearance of the Raman band at −3122 $cm^{-1}$.

To investigate the nature of the reagent ordering in the zeolite pores, we compare the spectral anisotropy in differently oriented crystallographic segments, close to the crystal surface (Figure 2). The ZSM-5 crystals consist of optically anisotropic subunits[12] (Figure 2 a): four pyramidal side segments and two elongated pyramidal units (top and bottom). Here, the top and bottom segments have the same crystallo-

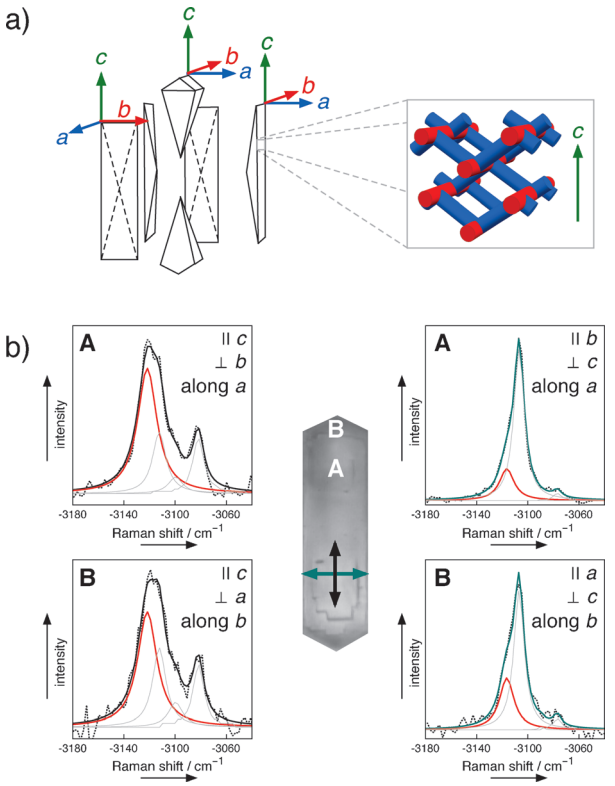


***Figure 2.*** a) Crystallographic subunits of ZSM-5; straight pores (inset, red) aligned along the crystallographic *b* axis; the normal of zigzag pores (inset, blue) along the *a* axis. b) mCARS responses (spectra (dotted) and fits (solid)) of 2CT/H-ZSM-5 obtained close to the surface of the crystal at positions A and B, which correspond to different crystallographic segments, normalized to the maximum band intensity. The Lorentz fit of the −3122 $cm^{-1}$ band is displayed in red; the thin black lines are Lorentz fits of the other CH stretching modes. Beam polarization/propagation as annotated.

graphic orientation as the side parts, while the front and back segments are rotated by 90° around the *c* axis. Straight pores run parallel to the *b* axis and the zigzag pore normal runs parallel to the *a* axis. Location A in Figure 2 is structurally equivalent to that probed in Figure 1: the beam propagates along *a*, and the response is probed perpendicular (top left) or parallel (top right) to *b*. At location B, the beam propagates along *b* and is polarized perpendicular (bottom left) or parallel (bottom right) to *a*. Because the signal-to-noise ratio in the CH region is higher than that in the CC region, we examine the behavior of the $-3122\ cm^{-1}$ band. This mode exhibits the same anisotropy pattern as ν(C-C) (rotated by 90° with respect to ν(C=C)). Lorentz fits of the $-3122\ cm^{-1}$ band are displayed in red; the thin black lines are the corresponding fits of the other CH resonances. Each spectrum is normalized with respect to its maximum band intensity. The responses at location B are qualitatively similar to those at A. This observation can be explained by a high degree of similar ordering of 2CT in both straight and zigzag pores. As the zigzag pores run at approximately 34° off the crystal's *a* axis, the intensity differences for probing parallel or perpendicular to *a* are expected to be less pronounced than for probing parallel or perpendicular to *b*. For the $-3122\ cm^{-1}$ mode, rotating the polarization causes an intensity difference at location A that is 50% larger than that at location B, increasing from 0.44 to 0.66. The normalized intensity of the $-3122\ cm^{-1}$ band increases from 0.19 $\parallel b$, along $a < 0.33 \parallel a$, along $b \ll 0.77 \perp a$, along $b < 0.85 \perp b$, along *a*. This order is consistent with the observations in Figure 1 in which the intensities are minimum for $\parallel b$ and maximum for $\perp b$ for ν(C–C), and the reverse for ν(C=C). Thus, while the (sub)micrometer spatial resolution of mCARS does not allow direct distinction between 2CT located in straight or in zigzag pores, probing different crystallographic segments of the zeolite provides insight into the adsorption geometry in the different pore types.

From these results, we deduce that the (subtle) differences in the Raman responses at different locations in the zeolite, which are attributed to the ordering of molecules in the pores, can be used to visualize the anisotropy of the crystal's pore structure in 3D. Note that in contrast to conventional, linear microscopy techniques, mCARS sections the chemical-optical properties of the sample with an intrinsic axial resolution of approximately 1.5 µm. Figure 3a displays 2D maps reconstructed from the band intensity of the $-3122\ cm^{-1}$ band relative to the maximum spectral intensity. Consecutive maps were recorded with voxel spacing of 2 µm. The beam polarization was ⊥ to the *c*-axis, with the light propagating in the direction of the roof ridge (left) or ⊥ to the roof ridge (right). The observed distributions of relative band intensities are spatially inhomogeneous at different crystal depths. For a crystal viewed along its roof ridge (Figure 3a, left), we find strong signals in the roof at all depths, while in the body of the crystal, the intensity grows in from all sides at the same time. For a crystal viewed perpendicular to its roof ridge (Figure 3a, right), only a weak response is recorded from the roof, and the intensity grows in from the long sides of the crystal when moving down towards the center plane. The observed

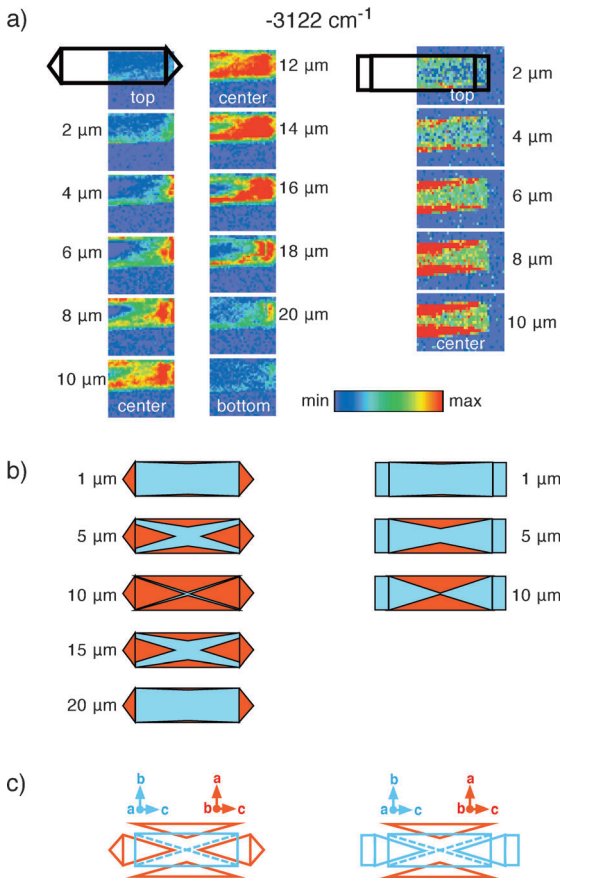


***Figure 3.*** a) Observed patterns of the relative intensity of the $-3122\ cm^{-1}$ band in 2D slices of 2CT/H-ZSM-5 viewed along the roof top (left) or perpendicular to the roof top (right), moving down from the top to the center to the bottom of the crystal with a step size of $\Delta z = 2$ µm; beam polarization perpendicular to the *c* axis. b) Expected intensity patterns for the respective beam polarizations with respect to the orientation of the zeolite's subunits as depicted in (c).

patterns display the segmented structure of the ZSM-5 particle (Figure 3c).

Taking into account the constraints imposed by the independent information about molecular ordering and pore orientation, we set out to determine the 2CT orientation. Figure 4 compares sketches of three possible geometries for adsorption of the reagent in the straight pores. We consider two extreme cases where head-to-tail dipolar chains (the 2CT dipole vector points largely toward the S atom)[13] are aligned with their molecular plane either in the *ab* plane (model A) or in the *bc* plane (model B) of the zeolite. Alternatively, a π-stacking configuration could be envisioned with the molecular plane parallel to the *ca* plane of the crystal (model C). To the right of the models, the expected Raman band activities for the C–C stretching modes are illustrated for beam polarizations parallel (black) or perpendicular (blue) to the crystal's *c* axis. The intensity of ν(C=C) is strongest when the excitation beam is polarized parallel to the straight pores (Figure 1a). This observation is in line with C=C bonds being oriented parallel to the straight pores, corresponding to a head-to-tail long-range order of 2CT (model A or B). While the π stacking of 2-substituted thiophenes was found to be the

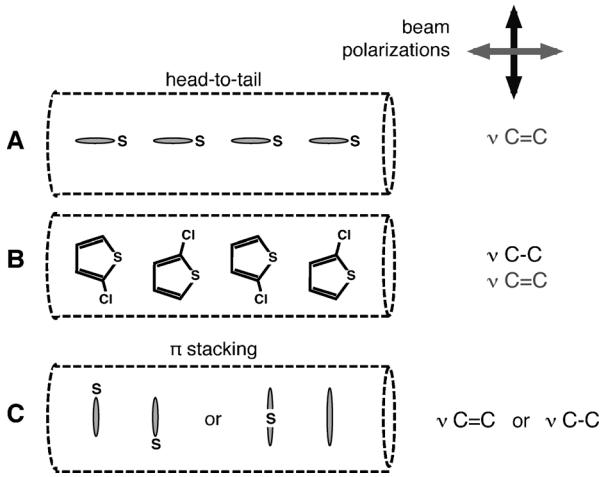


***Figure 4.*** Left: Sketches of selected possible adsorption geometries of long-range-ordered 2CT in straight pores. Model A: 2CT head-to-tail with the molecular plane in the *ab* plane of the zeolite. Model B: 2CT head-to-tail with the molecular plane in the *bc* plane of the zeolite. Model C: 2CT π stacking with the molecular plane in the *ca* plane of thee zeolite. Right: Expected Raman activities for beam polarizations parallel (black) or perpendicular (blue) to the *c* axis.

most favorable interaction in the solid state,[14] here the confinement of 2CT molecules inside the zeolite pores and their nonnegligible dipole moment of 1.65 D[13,15] likely render head-to-tail alignment the most favorable adsorption geometry. Similar chain formation has been observed previously for molecules with large permanent dipole moments such as *p*-nitroaniline (6.2 D)[16] and for elongated reaction products of styrene or thiophene oligomerization in zeolite pores.[3d,6] The 90° difference between the scattering lobes of ν(C=C) and ν(C−C) (Figure 1e,f) agrees best with 2CT alignment according to model B. Apparently, the elliptical pore structure and spatial constraint have a microscopic ordering effect on the orientation of the molecular chain, with 2CT rings preferably arranged in the crystal's *bc* rather than *ab* plane.

Note that for model B, when the beam propagates along the *b* axis, contributions from 2CT in the straight pores are expected to be negligible. The same is true for probing along *a*, albeit to a lesser extent, because the zigzag pores run 34° off the *a* axis. Hence, model B also explains the observed order of intensities of the $-3122\ cm^{-1}$ band as discussed above: Probing along *a*, $\parallel b$ contains a negligible signal contribution from the zigzag pores and only minor contributions from straight pores which results in the smallest overall band intensity; probing along *b*, $\parallel a$ results in an only slightly stronger signal with the main contribution from zigzag pores at 34° to the beam polarization. Probing along *b*, $\perp a$ gives a visibly more intense signal whose main contribution stems from zigzag pores at 56° to the beam polarization. The largest intensity is observed for probing along *a*, $\perp b$ to which 2CT in the straight pores contributes most.

According to model B, we expect the following 2D intensity patterns (Figure 3b): High relative band intensities (red) are expected in regions where, on account of the crystallographic orientation of the zeolite's subunits (Figure 3c), we probe $\parallel a$, while lower ones (blue) are expected when the excitation beams are polarized $\parallel b$. Notably, the observed patterns (Figure 3a) are in excellent agreement with the expected ones (Figure 3b). As a result, the 2D maps directly visualize the differently oriented segments of the zeolite, that is, its structural anisotropy, in 3D through the mCARS response of the ordered 2CT molecules; the generally accepted crystallographic model for coffin-shaped ZSM-5 crystals is confirmed.

In summary, we have demonstrated that mCARS serves as a valuable tool for the 3D characterization of the local geometric structure of both the reagent and the zeolite crystal at the sub-micrometer scale. Polarization-dependent measurements reveal the formation of 1D chains of adsorbate molecules following the pore structure and the spectral signatures of intermolecular dipole interactions, which, in combination with the spatial constraint of the zeolite pore geometry, explain the molecular arrangement. The approach is further used to visualize the structural anisotropy of ZSM-5 crystals with (sub)micrometer resolution in 3D, confirming that the employed ZSM-5 crystals are composed of six single-crystal subunits. Future experiments may help not only to elucidate the role of various parameters like temperature, solvent, and functional groups within the reagent molecules, but also to provide kinetic information on, for example, the diffusion of reactants within the pores.

Received: September 12, 2011
Published online: November 11, 2011

**Keywords:** CARS spectroscopy · microscopy · zeolites

[1] a) A. Bhan, E. Iglesia, *Acc. Chem. Res.* **2008**, *41*, 559–567; b) R. A. Schoonheydt, B. M. Weckhuysen, *Phys. Chem. Chem. Phys.* **2009**, *11*, 2794–2798; c) J. Kärger, P. Kortunov, S. Vasenkov, L. Heinke, D. R. Shah, R. A. Rakoczy, Y. Traa, J. Weitkamp, *Angew. Chem.* **2006**, *118*, 8010–8013; *Angew. Chem. Int. Ed.* **2006**, *45*, 7846–7849.

[2] S. Deore, P. Simoncic, A. Navrotsky, *Microporous Mesoporous Mater.* **2008**, *109*, 342–349.

[3] a) F. Schüth, *J. Phys. Chem.* **1992**, *96*, 7493–7496; b) F. Marlow, K. Hoffmann, W. Hill, J. Kornatowski, J. Caro, *Stud. Surf. Sci. Catal.* **1994**, *84*, 2277–2284; c) S. Megelski, A. Lieb, M. Pauchard, A. Drechsler, S. Glaus, C. Debus, A. Meixner, G. Calzaferri, *J. Phys. Chem. B* **2001**, *105*, 25–35; d) M. H. F. Kox, E. Stavitski, B. M. Weckhuysen, *Angew. Chem.* **2007**, *119*, 3726–3729; *Angew. Chem. Int. Ed.* **2007**, *46*, 3652–3655; e) D. Mores, J. Kornatowski, U. Olsbye, B. M. Weckhuysen, *Chem. Eur. J.* **2011**, *17*, 2874–2884.

[4] a) E. Fois, G. Tabacchi, G. Calzaferri, *J. Phys. Chem. C* **2010**, *114*, 10572–10579; b) C. Tuma, J. Sauer, *Angew. Chem.* **2005**, *117*, 4847–4849; *Angew. Chem. Int. Ed.* **2005**, *44*, 4769–4771.

[5] a) A. Gasecka, L. Q. Dieu, D. Bruehwiler, S. Brasselet, *J. Phys. Chem. B* **2010**, *114*, 4192–4198; b) M. A. van der Veen, B. F. Sels, D. E. de Vos, T. Verbiest, *J. Am. Chem. Soc.* **2010**, *132*, 6630–6631.

[6] M. H. F. Kox, K. F. Domke, J. P. R. Day, G. Rago, E. Stavitski, M. Bonn, B. M. Weckhuysen, *Angew. Chem.* **2009**, *121*, 9152–9156; *Angew. Chem. Int. Ed.* **2009**, *48*, 8990–8994.

[7] a) M. Zimmerley, R. Younger, T. Valenton, D. C. Oertel, J. L. Ward, E. O. Potma, *J. Phys. Chem. B* **2010**, *114*, 10200–10208; b) H. A. Rinia, G. W. H. Wurpel, M. Müller, *Methods Mol. Biol.*

**2007**, *400*, 45 – 61; c) G. W. H. Wurpel, H. A. Rinia, M. Müller, *J. Microsc.* **2005**, *218*, 37 – 45; d) J. Cheng, S. Pautot, D. Weitz, X. Xie, *Proc. Natl. Acad. Sci. USA* **2003**, *100*, 9826 – 9830.

[8] J. P. R. Day, K. F. Domke, G. Rago, H. Kano, H. Hamaguchi, E. M. Vartiainen, M. Bonn, *J. Phys. Chem. B* **2011**, *115*, 7713 – 7725.

[9] a) K. M. Mukherjee, T. N. Misra, *Spectrochim. Acta Part A* **1997**, *53*, 1439 – 1444; b) T. D. Klots, R. D. Chirico, W. V. Steele, *Spectrochim. Acta Part A* **1994**, *50*, 765 – 795; c) C. L. Garcia, J. A. Lercher, *J. Mol. Struct.* **1993**, *293*, 235 – 238; d) G. Paliani, R. Cataliotti, *Spectrochim. Acta Part A* **1981**, *37*, 707 – 710; e) M. Horak, I. J. Hyams, E. R. Lippincott, *Spectrochim. Acta* **1966**, *22*, 1355 – 1363.

[10] K. Hoffmann, U. Resch-Genger, F. Marlow, *Microporous Mesoporous Mater.* **2000**, *41*, 99 – 106.

[11] T. Danno, J. Kürti, H. Kuzmany, *Phys. Rev. B* **1991**, *43*, 4809 – 4819.

[12] L. Karwacki, M. H. F. Kox, D. A. M. de Winter, M. R. Drury, J. D. Meeldijk, E. Stavitski, W. Schmidt, M. Mertens, P. Cubillas, N. John, A. Chan, N. Kahn, S. R. Bare, M. Anderson, J. Kornatowski, B. M. Weckhuysen, *Nat. Mater.* **2009**, *8*, 959 – 965.

[13] H. S. I. Beigi, S. Jameh-Bozorghi, *Chem. Cent. J.* **2011**, *5*, 13.

[14] S. Tsuzuki, K. Honda, R. Azumi, *J. Am. Chem. Soc.* **2002**, *124*, 12200 – 12209.

[15] R. Keswani, H. Freiser, *J. Am. Chem. Soc.* **1949**, *71*, 218 – 220.

[16] F. Marlow, W. Hill, J. Caro, G. Finger, *J. Raman Spectrosc.* **1993**, *24*, 603 – 608.

Supporting Information

© Wiley-VCH 2011

69451 Weinheim, Germany

# Host–Guest Geometry in Pores of Zeolite ZSM-5 Spatially Resolved with Multiplex CARS Spectromicroscopy**

*Katrin F. Domke,* James P. R. Day, Gianluca Rago, T. Alexander Riemer, Marianne H. F. Kox, Bert M. Weckhuysen, and Mischa Bonn*

anie_201106447_sm_miscellaneous_information.pdf

# Supporting Information

*Zeolites*

ZSM-5 crystals (Si/Al ratio of ~ 20) were obtained from Exxon-Mobil (Machelen, Belgium). They were converted into their acid form by triple ion-exchange with a 10 wt% ammonium nitrate solution and subsequent calcination at 823 K. 2-chloro-thiophene (2CT) was used as received (Sigma-Aldrich). Crystals were immersed in ca. 8 μL of 2CT and analyzed after excess 2CT had evaporated.

*mCARS Experimental details*

The coffin-shaped (H- or Na-) ZSM-5 crystals (ca. 20 x 20 x 100 $\mu m^3$, Si/Al = 20) containing straight pores (5.4 x 5.6 $Å^2$) connected by zigzag pores (5.1 x 5.5 $Å^2$, opening angle of 112.6°)[S1] were fully loaded with 2CT and inspected with mCARS. The scattering intensities were analysed as a function of crystal orientation relative to the beam polarization (probing $\chi^{(3)}_{1111}$ with Stokes/pump/probe/ CARS fields parallel to each other[S2]).

Our multiplex CARS set-up consists of two tunable mode-locked Ti:sapphire lasers (Tsunami, Spectra Physics) with a repetition rate of 80 MHz, pumped by a 532 nm Nd:YVO4 laser (Millenium, Spectra Physics). The pump laser was centered at 707 nm and generated pulses of 10 ps (bandwidth ~ 1.5 $cm^{-1}$, at full width half maximum, fwhm). The Stokes laser produced 80 fs pulses (bandwidth ~ 180 $cm^{-1}$, fwhm) and was centered at 910 nm to probe molecular vibrations with Raman shifts in the CH-stretch region and at 790 nm to probe the -1300 to -1500 $cm^{-1}$ CC stretch region. The two beams were adjusted to be collinear and synchronized (Lok-to-Clock®, Spectra Physics) to establish the spatial and temporal overlap necessary for the generation of CARS. An additional, home-built feedback system stabilized the long-term time jitter between the laser pulses below 1 ps. The zeolite crystals loaded with 2CT were placed between two 150 μm thick glass cover slips, and the sample was mounted vertically in the mCARS set-up. The overlapping laser beams were focussed on the sample with an oil-immersion microscope objective (1.3 NA, 40x, Zeiss Plan-Neofluar). The scattered light was collected with an air-immersion objective (0.65 NA, 40x, Zeiss A-Plan) in forward direction and was filtered by a 710-nm short-pass filter (Omega Optical) and a 710-nm notch filter (Kaiser Optical Systems) before entering the

spectrograph (Oriel MS 257, 5 $cm^{-1}$ spectral resolution). mCARS spectra were recorded with a CCD camera (Andor V420-OE). The piezo-driven sample stage allowed movement of the zeolite sample through the laser focus and thus the recording of 3D maps. The CARS focus had been measured previously to be ~ 300 nm in x,y- and ~ 1 μm in z-direction.[S3] For the study reported here, the piezo step size was set to 2 μm in x,y,z-directions. The integration time was 0.5 s per point.

Placing polarizers in the pump and Stokes beam paths and a λ/2 wave plate plus analyzer in the collection beam path allowed us to adjust the beam polarizations of pump/probe beams to be parallel to the Stokes/CARS beams to probe only the $\chi^{(3)}_{1111}$ tensor elements. The polarization of the scattered beam entering the spectrograph was set to be vertical to ensure uniform detection sensitivity. The error in alignment amounted to ±3° for the crystal orientation (sample holder rotation stage and manual error) and ±1° for the beam polarizations (polarizer precision).

After dividing the spectra by a non-resonant reference spectrum (glass cover slip), the resulting normalized data were analysed by applying the Maximum Entropy Method (MEM).[S4] This mathematical analysis procedure allows us to retrieve the imaginary part of the resonant contribution to the third-order nonlinear susceptibility of the sample, $Im\chi^{(3)}$, which is, in the case of probing $\chi^{(3)}_{1111}$, comparable to the normal Raman response of the system and to which we refer as Raman response throughout the manuscript. This Raman-like response allows for direct quantitative analysis.

[S1] D.H. Olson, G.T. Kokotailo, S.L. Lawton, W.M. Meier, *J. Phys. Chem.* **1981**, *85*, 2238-2243.

[S2] M.D. Levenson, *J. Raman Spectrosc.* **1981**, *10*, 9-23.

[S3] G.W.H. Wurpel, J.M. Schins, M. Müller, *Optics Lett.* **2002**, *27*, 1093-1095.

[S4] E. Vartiainen, K.-E. Peiponen, H. Kishida, T. Koda, J. Opt. Soc. Am. B **1996**, *13*, 2106-2114.

*Supplementary Results*

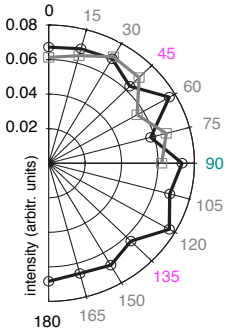


***Figure S1.*** Two independent control experiments (grey squares and black circles) probing the $N_2$ stretch vibration of nitrogen (air) adsorbed inside the zeolite pores. The Raman response shows no anisotropy when varying the angle between beam polarization and crystal's *c*-axis. See main text for details.

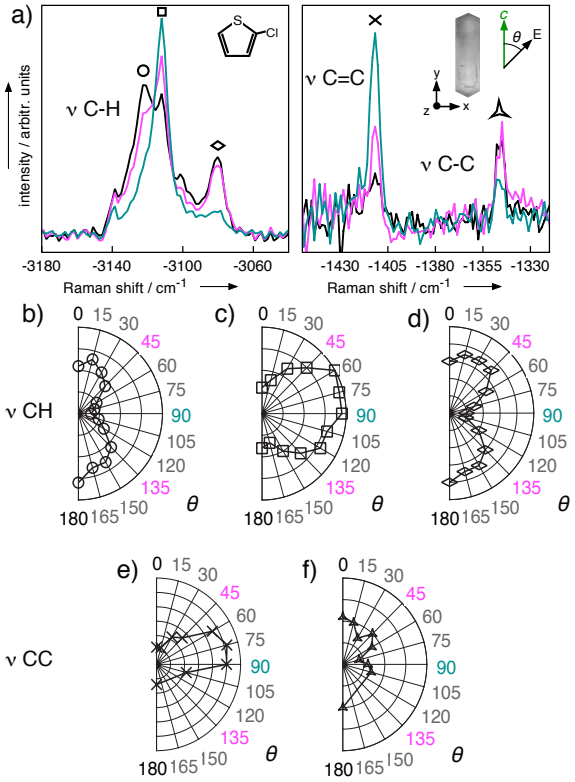


***Figure S2.*** Varying the angle $\theta$ between the crystal's *c*-axis and the beam polarization results in changes in the Raman response of 2CT/H-ZSM-5. At $\theta$ = 0°, the beam polarization is aligned ⊥ to the straight pores. a) Example spectra recorded at a depth z = 8 µm centred in x,y in CH and CC stretch regions for $\theta$ = 0° (black), 45/135° (ma-

genta), 90° (blue). Insets: chemical structure of 2CT; beam polarization with respect to *c*-axis of crystal (white-light image of ZSM-5 crystal). b) to f) Polar plots of band intensities as a function of $\theta$: b) -3122, c) -3110, d) -3080, e) -1410, f) -1345 $cm^{-1}$.

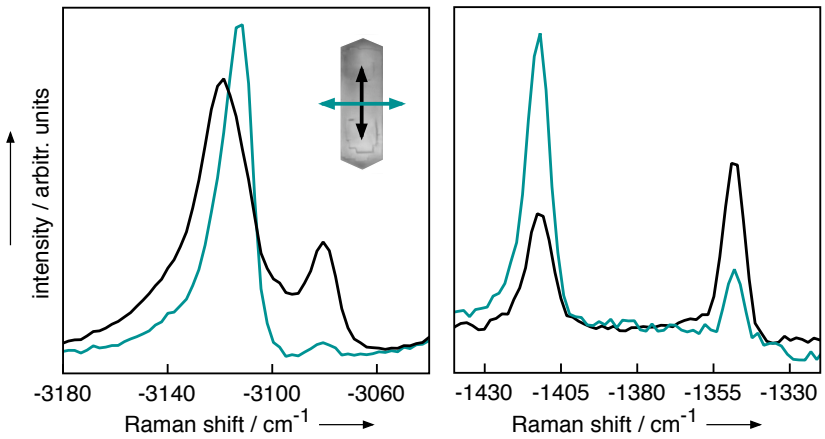


***Figure S3.*** Raman response in the CH (left) and CC (right) regions of 2CT/Na-ZSM-5. Rotating the beam polarization with respect to the *c*-axis of the crystal results in similar spectral changes as observed for 2CT/H-ZSM-5. See main text for details.